Detection of the secondary meridional circulation associated with the quasi-biennial oscillation

P. Ribera,[1] C. Peña-Ortiz,[1] R. Garcia-Herrera,[2] D. Gallego,[1] L. Gimeno,[3] and E. Hernández[2]

Received 18 November 2003; revised 11 June 2004; accepted 22 June 2004; published 23 September 2004.

[1] The quasi-biennial oscillation (QBO) signal in stratospheric zonal and meridional wind, temperature, and geopotential height fields is analyzed based on the use of the National Centers for Environmental Prediction (NCEP) reanalysis (1958–2001). The multitaper method-singular value decomposition (MTM-SVD), a multivariate frequency domain analysis method, is used to detect significant and spatially coherent narrowband oscillations. The QBO is found as the most intense signal in the stratospheric zonal wind. Then, the MTM-SVD method is used to determine the patterns induced by the QBO at every stratospheric level and data field. The secondary meridional circulation associated with the QBO is identified in the obtained patterns. This circulation can be characterized by negative (positive) temperature anomalies associated with adiabatic rising (sinking) motions over zones of easterly (westerly) wind shear and over the subtropics and midlatitudes, while meridional convergence and divergence levels are found separated by a level of maximum zonal wind shear. These vertical and meridional motions form quasi-symmetric circulation cells over both hemispheres, though less intense in the Southern Hemisphere. *INDEX TERMS:* 3334 Meteorology and Atmospheric Dynamics: Middle atmosphere dynamics (0341, 0342); 3319 Meteorology and Atmospheric Dynamics: General circulation; 3314 Meteorology and Atmospheric Dynamics: Convective processes; *KEYWORDS:* QBO, secondary meridional circulation, stratosphere dynamics

Citation: Ribera, P., C. Peña-Ortiz, R. Garcia-Herrera, D. Gallego, L. Gimeno, and E. Hernández (2004), Detection of the secondary meridional circulation associated with the quasi-biennial oscillation, *J. Geophys. Res.*, *109*, D18112, doi:10.1029/2003JD004363.

1. Introduction

[2] The secondary meridional circulation (SMC) associated with the quasi-biennial oscillation (also called "direct quasi-biennial oscillation (QBO) circulation") was first described by *Reed* [1964]. In 1982, *Plumb and Bell* [1982] performed the first detailed two-dimensional (2-D) model analysis of its latitudinal and vertical structure. The SMC consists of a modulation of the stratospheric mean meridional circulation, also called Brewer-Dobson circulation, produced by the QBO. This circulation is characterized by air rising at low latitudes, a poleward drift, and a sinking at higher latitudes [*James*, 1994]. Thus understanding the effects of the QBO in the global stratospheric circulation is essential to understanding the underlying dynamics and the temperature and tracer distribution in the stratosphere.

[3] The SMC is characterized by a sinking motion at the equator in westerly shear zones and rising in easterly shear areas. A maximum (minimum) in temperature at the equator in westerly (easterly) shear zones is necessary to maintain the thermal wind balance. The sinking (rising) motions produce adiabatic heating (cooling) to preserve positive and negative temperature anomalies against thermal damping [*Baldwin et al.*, 2001]. As *Plumb and Bell* [1982] illustrated in their 2-D model, the SMC is also distinguished by meridional convergence (divergence) zones over the equator coinciding with the location of maximum westerly (easterly) wind. The QBO temperature anomaly changes sign at approximately ±15° owing to rising (sinking) motions that compensate the sinking (rising) motions at the equator [*Cordero and Nathan*, 2000; *Baldwin et al.*, 2001; *Choi et al.*, 2002].

[4] Although the SMC was initially considered confined between 30°S and 30°N [*Plumb and Bell*, 1982], some authors have pointed out that it is not restricted to the tropical area and affects temperature and tracers in the extratropics and midlatitudes as well [*Gray et al.*, 2001; *Baldwin et al.*, 2001; *Kinnersley and Tung*, 1998]. Recent studies have suggested that the latitudinal extension of these circulation cells is seasonally dependent, reaching middle and high latitudes in winter and spring. The most widely accepted idea is that extratropical QBO influence occurs through the modulation of extratropical Rossby waves. Additionally, some authors have pointed out the possibility that other dynamical mechanisms could also participate in the meridional propagation of the QBO signal through

[1]Departamento de Ciencias Ambientales, Universidad Pablo de Olavide, Sevilla, Spain.
[2]Departamento Fisica de la Tierra II, Universidad Complutense de Madrid, Madrid, Spain.
[3]Departamento Fisica Aplicada, Universidad de Vigo, Ourense, Spain.

0148-0227/04/2003JD004363

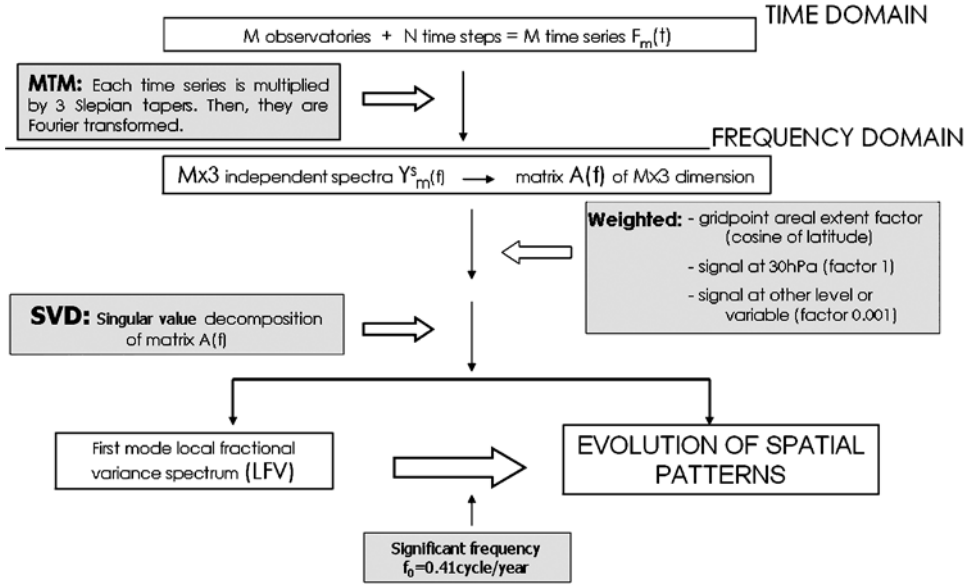

Figure 1. Schematic diagram of the MTM-SVD methodology.

interactions with the Brewer-Dobson circulation, which could be another factor in the poleward propagation of the SMC and the QBO ozone anomaly [*Kinnersley and Tung*, 1998, 1999].

[5] The SMC has been extensively studied directly with models and indirectly through its effects in the distribution of dynamic variables such as potential vorticity or tracers such as CH_4, H_2O, N_2O, NO_2, O_3, and aerosols. However, its direct observation is very difficult, and the current studies of the mean meridional circulation in the stratosphere do not evidence any signal of QBO modulations, probably because of the low meridional and vertical wind speed involved [*Choi et al.*, 2002; *Huesmann and Hitchman*, 2001].

[6] The multitaper method–singular value decomposition (MTM-SVD) method [*Mann and Park*, 1999] has been used to detect the SMC from the National Centers for Environmental Prediction–National Center for Atmospheric Research (NCEP-NCAR) reanalysis. It is applied to isolate spatially coherent patterns of narrowband variability present in stratospheric zonal wind and other climate fields simultaneously. After the QBO is detected as the only coherent source of oscillatory variability on interannual timescales, its signal is projected onto other data fields, such as the meridional wind, temperature, and geopotential height. Then, MTM-SVD is used to reconstruct the spatial and temporal patterns of meridional wind, temperature, and geopotential height associated with the equatorial zonal wind QBO. With this procedure a picture of SMC is clearly depicted.

2. Data and Method

[7] In this study, 1958–2001 monthly data of zonal and meridional wind, geopotential height, and temperature at multiple stratospheric levels (200, 150, 100, 70, 50, 30, 20, and 10 hPa) from the NCEP-NCAR reanalysis have been used [*Kalnay et al.*, 1996; *Kistler et al.*, 2001]. The spatial resolution of the data is 5° latitude by 5° longitude, covering the whole globe (90°N and 90°S not included), including a total number of 2520 grid points per level. Monthly grid point data were deseasonalized, converted into standardized anomalies, and then weighted by a grid point areal extent factor (cosine of latitude).

[8] The MTM-SVD is initially applied to the zonal wind anomaly data set at different pressure levels in the stratosphere. A schematic diagram of this procedure is represented in Figure 1. Each standardized time series $Fm(t)$ for each grid point is transformed from the time to the spectral domain through the MTM procedure. The MTM is a spectral analysis method used to examine a temporal sequence of data in terms of its frequency content. Each time series, $Fm(t)$, is multiplied by the first three orthogonal Slepian data tapers in order to reduce the spectral leakage (see *Venegas* [2001] and *Percival and Walden* [1993] for details). Each of these three time series obtained for each grid point is then Fourier transformed. An $M \times 3$ (where M is the total number of observatories) dimension matrix $A(f)$ is constructed with the three independent spectra obtained for the time series, $Y_{sm}(f)$, where m and s are the observatory (from 1 to 2520) and data taper (from 1 to 3), respectively. An SVD is performed for $A(f)$ at each frequency f from zero to the Nyquist frequency. The left and right singular vectors ($\mathbf{U_m^k}$ and $\mathbf{V_s^k}$, respectively) obtained represent the temporal and spatial patterns of the signal associated with a given frequency. The complex vector $\mathbf{U_m^k}(f_0)$ of dimension m is the spatial pattern corresponding to the k mode of the decomposition at f_0. It contains information about relative phase and amplitude of the signal at all locations m. On the other hand, the complex vector $\mathbf{V_s^k}$ gives information about the amplitude and phase modulations on a timescale longer than the oscillation period [*Venegas*, 2001]. The singular values obtained are proportional to the variance associated with the temporal and spatial patterns obtained for each mode. The largest singular value represents the maximum variance contained

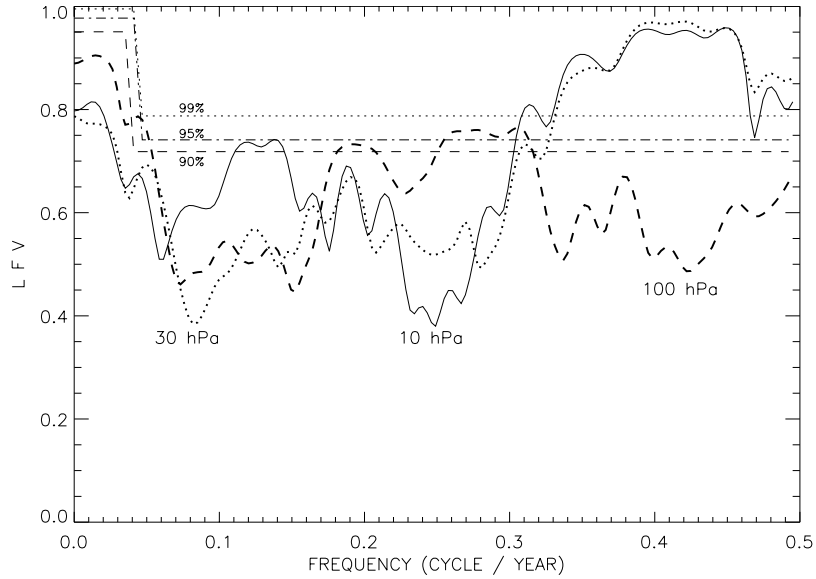

Figure 2. Local fractional variance (LFV) spectrum (1958–2001) with 90, 95, and 99% significance level for 10, 30, and 100 hPa zonal wind fields.

in the spatial and temporal patterns obtained for each frequency. The largest singular values can be expressed as a function of frequency to construct the local fractional variance (LFV) spectrum, used to identify significant oscillatory bands [*Mann and Park*, 1999]. A Monte Carlo test is performed to determine statistical significance levels. One thousand different combinations of the temporal intervals are used to generate 1,000 randomized versions of the field F which conserve the spatial but not the temporal structure. Statistical significance levels are thus obtained by taking the 90, 95, and 99 percentiles of this set of fields F.

[9] After this analysis the QBO arises as the most intense signal (with a mean period of 28 months) found in the zonal wind anomaly data set, the signal being most intense at 30 hPa (Figure 2). Thus, in this paper, the 30 hPa signal is projected on every other stratospheric level and variable (temperature, meridional wind, and geopotential height) to obtain the spatial and temporal patterns induced over them by the QBO. Again, the MTM-SVD method is used to determine these projections and the associated patterns. During this procedure the time series of the different variables are transformed into the frequency domain using the same three tapers, and the resulting spectra of the fields are merged in pairs (30 hPa zonal wind plus other field) to form matrices $A(f)$ of $2M \times 3$ dimension. The new matrices were then weighted to separate the QBO signal from its projections. This is done by using the cosine of latitude areal factor for zonal wind at 30 hPa and the same areal factor multiplied by a highly reducing factor (0.001) for all the other fields (every other variable and/or pressure level) (see *Mann and Park* [1999], *Venegas* [2001], and *Ribera and Mann* [2002, 2003] for details). The objective of this weighting is to isolate the QBO signal during the subsequent singular value decomposition of the weighted matrix, which is performed in the same way as the SVD previously described. Finally, the joint variability between the zonal wind signal associated with the QBO and the meridional wind, temperature, or geopotential height are analyzed through the obtained patterns. In order to analyze the meridional and vertical structures of these patterns, the resulting data fields (associated with the different variables) were zonally averaged for every pressure level to take the Eulerian mean. In this way, vertical profiles of the mean meridional patterns can be analyzed through a complete QBO cycle.

3. Analysis

[10] The LFV spectra performed for the zonal wind fields at every pressure level (from 10 to 200 hPa) show a broad band of statistically significant variability with periods ranging from 2 to 3 years (from $F = 0.33$ to $F = 0.45$ cycles per year) in levels from 10 to 70 hPa. Examples of these LFV spectra are included in Figure 2. Higher levels (10 and 30 hPa) are characterized by significant oscillatory bands between 0.33 and 0.45 cycles/year, while lower levels (100 hPa) are not. This is consistent with the mean period (28 months) described by previous studies as the most characteristic for the QBO during the second half of the twentieth century [*Maruyama*, 1997; *Huesmann and Hitchman*, 2001; *Hamilton and Hsieh*, 2002]. The most intense QBO signal is found at 30 hPa (Figure 2), and the frequency chosen to represent the oscillation is that with the maximum variance at this level (0.41 cycles/year). The mean zonal vertical and latitudinal structure of the QBO signal in zonal wind, meridional wind, temperature, and geopotential height and its temporal evolution are shown in Figure 3. The temporal evolution of the associated spatial patterns is represented through the use of five consecutive phases, beginning during the westerly QBO phase (phase 0°) and ending at the easterly QBO phase (phase 180°), with phase increments of 45°. Anomalies at 180° are, by construction, opposite to those observed at phase 0°.

3.1. QBO Signal in Zonal Wind

[11] Figure 3a, where the zonal wind is represented, is characterized by an intense QBO signal between 20°S and 20°N. At phase 0° the most intense westerly anomaly is located at 30 hPa, but 3 months later, during phase 45°, has

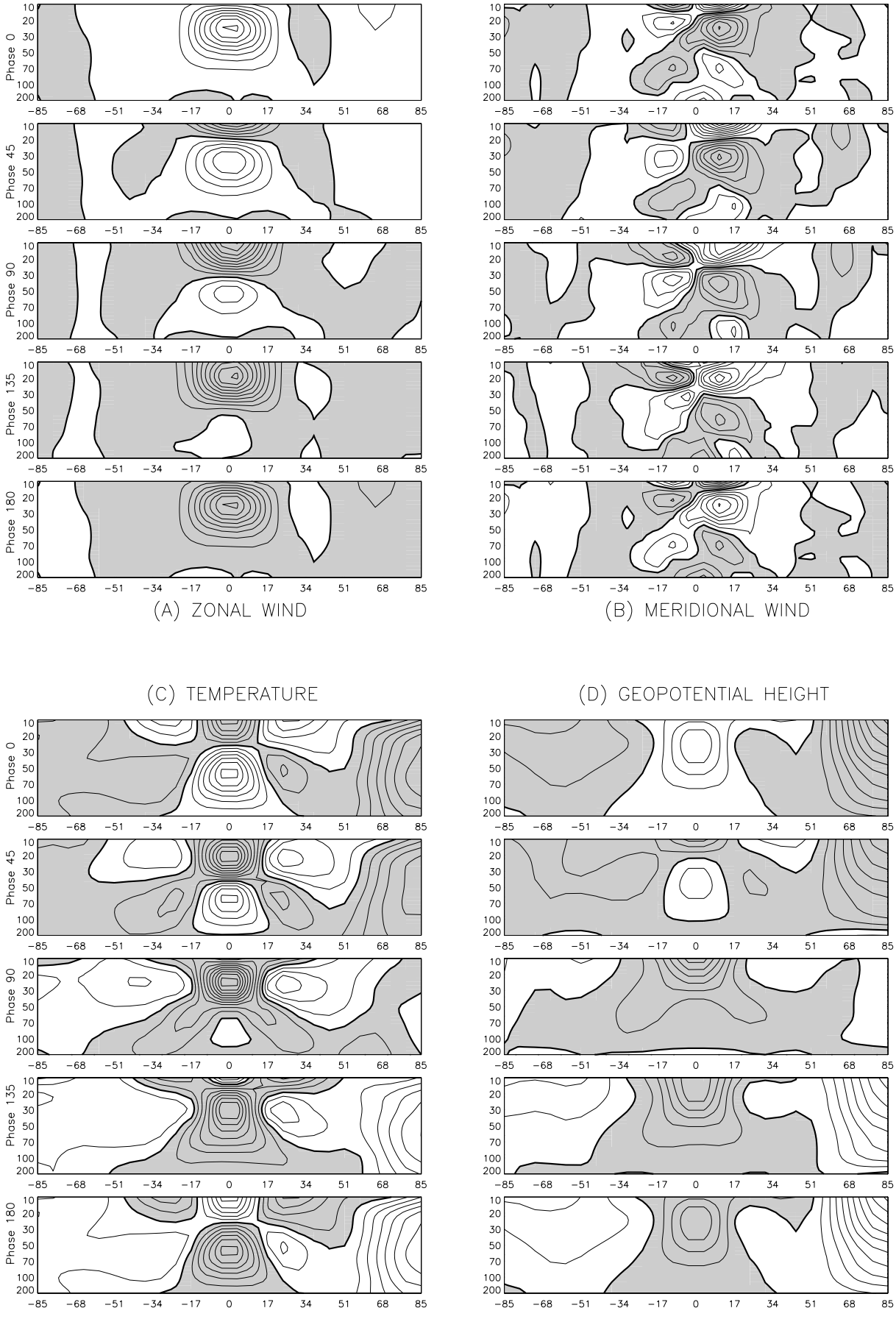
Phase 0
Phase 45
Phase 90
Phase 135
Phase 180
10 20 30 50 70 100 200
−85 −68 −51 −34 −17 0 17 34 51 68 85
(A) ZONAL WIND
(B) MERIDIONAL WIND
(C) TEMPERATURE
(D) GEOPOTENTIAL HEIGHT

Figure 3

descended to 50 hPa, while an intense easterly anomaly is observed at 10 hPa. A downward propagation of the easterlies from 10 hPa to 70/100 hPa is evident through the observation of the following phases. At phase 225°, intense westerly wind is evident above the easterlies (not shown). It propagates downward, completing the cycle when it again reaches the situation represented at phase 0°. This result is consistent with previous analysis of the QBO propagation in the tropical areas [*Naujokat*, 1986; *Hamilton*, 1998; *Gray et al.*, 2001; *Baldwin et al.*, 2001]. Over higher latitudes a clear asymmetry between the Northern and the Southern Hemisphere is evidenced. The modulation of the stratospheric polar vortex by the QBO is more intense in the Northern Hemisphere, where the westerly (easterly) QBO phase is associated with acceleration (deceleration) of the stratospheric polar vortex, than in the Southern Hemisphere. However, in the Southern Hemisphere the QBO signal over high latitudes is much weaker, while at lower latitudes it has larger extension. This is, again, consistent with previous descriptions of the QBO signal in the extratropics [*Baldwin and Dunkerton*, 1998, 1999, 2001; *Naito*, 2002; *Thompson et al.*, 2002].

3.2. QBO Signal in Meridional Wind and Temperature: The Secondary Meridional Circulation

[12] Figure 3b represents the QBO effects over the meridional wind. The main characteristic of the meridional circulation associated with the QBO is the existence of equatorial areas of convergence and divergence. Meridional convergence (divergence) is produced when a negative (positive) anomaly in the meridional wind in the Northern Hemisphere equatorial zone and a positive (negative) one in the Southern Hemisphere are simultaneously detected at the same level. The comparison of Figures 3a and 3b shows that the areas of largest u values (10–20 m/s) are associated with zones of meridional convergence (divergence) [*Choi et al.*, 2002; *Baldwin et al.*, 2001; *Cordero and Nathan*, 2000]. Out of the phases and zones where the maximum westerly and easterly wind reaches 10–20 m/s, the association between the meridional convergence (divergence) motion and the westerly (easterly) wind maximum is not observed. Thus, only at levels from 10 to 30 hPa, it is possible to establish the spatial coincidence of the maximum zonal wind and the convergence or divergence zones.

[13] At phase 0°, there is a westerly wind maximum at 30 hPa over the equatorial zone. At this phase the meridional convergence zone associated with the westerly wind is also located at 30 hPa. At phase 90° the equatorial westerly wind zone has descended, and its maximum is now centered between 50 and 70 hPa. The meridional convergence zone is upward displaced and is now located between 30 and 50 hPa. At phases 135° and 180°, when the westerlies are restricted to the lower stratosphere, there are still convergence zones centered at 50 and 70 hPa, respectively. A similar evolution is observed for the divergence/easterlies relationship between phases 180° and 360° (not shown). The convergence (divergence) zones do not exactly follow the descent of the westerlies (easterlies) maximum. Convergence and divergence levels are separated by a level of maximum zonal wind shear. For example, at phase 45° the most intense westerly flow is located at 40 hPa, the most intense easterly flow is over 10 hPa, and the maximum wind shear is at 20 hPa, separating both maxima. Thus for this phase the level of most intense convergence is centered at 40 hPa, coincident with the maximum westerly wind, and the divergence level is centered at 10 hPa, coincident with maximum easterly wind. On the other hand, for phase 135° the most intense westerly flow is at 90 hPa, and the maximum easterly flow is at 20 hPa, but the convergence is centered at 60 hPa, and the divergence is slightly below 20 hPa, with the maximum wind shear centered between 40 and 50 hPa.

[14] Figure 3b also shows that for all phases the most significant QBO anomalies in the meridional wind are located between ±20° latitude. However, positive (negative) and negative (positive) meridional wind anomalies, over the Northern and Southern Hemisphere, respectively, related to divergence (convergence) motions, do not change their sign until ±50° latitude in those phases characterized by the most intense westerlies (easterlies). This result suggests that the area influenced by the meridional convergence (divergence) motions reaches middle and high latitudes during strong QBO phases. These areas are restricted to ±20° latitude as the signal propagates downward, and the westerlies (easterlies) become less intense.

[15] Figure 3c represents temperature anomalies associated with the QBO. In the equatorial area, between 15°S and 15°N, positive (negative) temperature anomalies are observed over the westerly (easterly) shear zones. This is consistent with the warm (cold) anomalies required in the westerly (easterly) shear zones by the thermal wind balance, as is expressed by equation (1) for the equatorial β plane approximation of the thermal wind relationship [*Choi et al.*, 2002; *Baldwin et al.*, 2001]:

$$\frac{\partial \overline{u}}{\partial z} = \frac{-R}{H\beta}\frac{\partial^2 \overline{T}}{\partial y^2} \longrightarrow \delta \overline{T}_{\mathrm{QBO}} \approx \frac{L^2 H\beta}{R}\frac{\partial \overline{u}}{\partial z}, \qquad (1)$$

where z is the log pressure height, δT_{QBO} is the temperature anomaly associated with the QBO, L is the meridional scale of the QBO, H is the scale height, R is the gas constant for the air, $\overline{u}$ is the zonal mean of the zonal component of the wind, $\overline{T}$ is the zonal mean temperature, and y is latitude.

[16] Figure 3c also shows that the QBO influence on temperature is not restricted to the equatorial area; on the contrary, it shows that the QBO temperature signal is quasi-symmetric about the equator and has a phase reversal at about ±15° latitude. In midlatitudes (from ±15° to ±55°),

Figure 3. (a) Evolution of the latitudinal and vertical structure of the QBO signal in the zonal mean value of the zonal wind through five consecutive phases (0°, 45°, 90°, 135°, and 180°) from westerly to easterly phase. (b) As in Figure 3a but for meridional wind. (c) As in Figure 3a but for temperature. (d) As in Figure 3a but for geopotential height. Negative (shaded) and positive (white) anomalies are indicated. The distance between consecutive isolines is as follows: 2 m/s for zonal wind (Figure 3a), 15 cm/s for meridional wind (Figure 3b), 0.2 K for temperature (Figure 3c), and 10 m for geopotential height (Figure 3d).

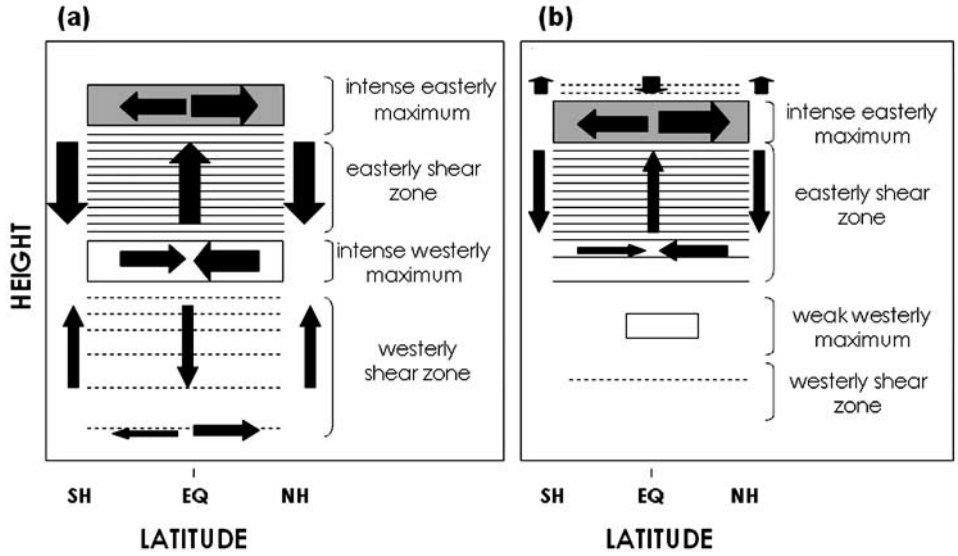

Figure 4. Schematic latitude-height sections showing the SMC most characteristic features. Arrows represent vertical and meridional wind, the intensity of the wind being proportional to the thickness of the arrow (vertical and meridional scales are independent). Westerly (dashed lines) and easterly (solid lines) shear zones are shown. A maximum in the easterly wind (shaded boxes) and the maximum westerly wind (white boxes) are shown. The intensity of the wind is represented by the area of the corresponding box. SH is Southern Hemisphere, EQ is equator, and NH is Northern Hemisphere. (a) Convergence/divergence at the same level as the westerly/easterly maximum. (b) Convergence or divergence not coinciding with westerly or easterly maximum.

opposite sign anomalies are found (cold and warm, respectively). These stratospheric warm (cold) temperature anomalies induced by the QBO are produced, and maintained against thermal damping, by adiabatic sinking (rising) motions [*Choi et al.*, 2002; *Baldwin et al.*, 2001]. In this way, positive (negative) temperature anomalies, represented in Figure 3c, are interpreted as a descent (ascent) of air. These results confirm the downward propagation of temperature anomalies following the descent of the QBO signal in the equatorial zonal wind.

[17] Over high latitudes, during the QBO westerly (easterly) phase, when inphase temperature is analyzed, colder (warmer) than normal conditions are observed over both polar regions, though they are more intense in the Northern Hemisphere (Figure 3c), as expected from previous studies [*Salby and Callaghan*, 2000; *Baldwin and Dunkerton*, 2001; *Ribera et al.*, 2003]. No significant meridional wind QBO anomalies are located at high latitudes.

[18] Finally, looking at results presented by *Huesmann and Hitchman* [2003], a shift in the NCEP reanalysis temperature and meridional wind data fields in 1978 has to be considered. Differences were detected in the anomalies of temperature and wind speed and in the meridional extension of the QBO area of influence over temperature. Thus the results might be affected by quantitative deviations; maximum absolute values of T (v) are probably lower (higher) than in reality. However, the evolution of the described patterns does not seem to be significantly modified.

3.3. QBO Signal in Geopotential Height

[19] Figure 3d shows the anomalies in the geopotential height associated with the QBO. At phase 0°, when the most intense westerly wind is detected, positive geopotential height anomalies are found over the equatorial region, while negative anomalies are detected over the poles. During the next phases, as the easterly wind appears above the westerlies and propagates downward, the positive geopotential height anomaly at the equatorial area turns into a negative anomaly while, over polar regions, negative anomalies become positive. Anomalies at the polar regions are less intense in the Southern Hemisphere than in the Northern Hemisphere but are characterized by a higher latitudinal extension [*Huesmann and Hitchman*, 2001; *Holton and Tan*, 1980].

[20] Positive (negative) anomalies in the geopotential height reflect an increase (decrease) of the thickness of the layer below a given level [*Holton*, 1972] and, consequently, proportional to its average temperature. Therefore positive (negative) anomalies in the geopotential height are also related to warm (cold) temperature anomalies in the layer below. This fact is evident in the obtained latitudinal and vertical structures of QBO temperature and geopotential height (Figures 3c and 3d).

3.4. A Picture of the Secondary Meridional Circulation

[21] The joint analysis of the previously described meridional motions and the vertical motions related to temperature anomalies provides a clear picture of the secondary meridional circulation. The existence of the convergence and divergence zones is directly related to the rising and sinking motions. Air mass continuity requires the succession of convergence and divergence areas for consecutive vertical levels; the upward (downward) transport of air mass produced by convergence (divergence) in lower levels has to be maintained by divergence (convergence) aloft (below). Large negative (positive) temperature

anomalies are found over zones of strong easterly (westerly) wind shear. To maintain these cold (warm) anomalies, air has to rise (sink), with the consequent adiabatic cooling (warming). Consequently, the convergence and divergence zones associated with the vertical motions are situated just below and above the zones of most intense zonal wind shear and temperature anomaly, which is consistent with the results shown in Figures 3b and 3c.

[22] The sinking and rising motions over the equatorial wind shear zones and over the subtropics and midlatitudes, added to the divergence and convergence motions, form circulation cells, quasi-symmetrical about the equator but less intense in the Southern Hemisphere. A schematic version of these cells at phases 45° and 135° is represented in Figures 4a and 4b, respectively. In Figure 4 the location of the maximum easterly and westerly QBO winds are represented together with wind shear layers and a schematic representation of the associated secondary meridional cells. As a general characteristic, for those cases where the intensity of successive easterly and westerly flows is very high, the cell circulation is more intense than for those cases where one of the zonal fluxes is not so intense. Thus in the first case (represented in Figure 4a) the associated meridional and vertical wind anomalies (expected from temperature anomalies) are higher than in the second case (represented in Figure 4b).

[23] In Figure 4a, there are two intense absolute zonal wind maxima (one from the west and one from the east) separated by a layer with a pronounced easterly wind shear, where a great air mass has risen. As previously explained, convergence and divergence are located at the vertical limits of this maximum shear layer. Thus for this case, convergence and divergence are located at the same level as the westerly and easterly maximum wind.

[24] Figure 4b represents those cases where a weak westerly maximum is accompanied by an intense easterly maximum. As a consequence, the lower vertical limit of the layer, where the maximum wind shear is observed, does not coincide with the weak westerly maximum. Thus in these cases, divergence is detected at the same level as easterly maximum, but convergence is displaced to the lower limit of the maximum wind shear layer, situated over the weak westerly maximum. A similar pattern would be detected for those cases where an intense westerly maximum is accompanied by a weak easterly maximum.

4. Summary and Conclusions

[25] The MTM-SVD methodology provides a detailed picture of the temporal evolution of the spatial patterns of several variables through a QBO cycle. The analysis of the QBO modulation of the meridional wind shows the existence of meridional convergence and divergence zones over the equator, located at the lower and upper limits of maximum zonal wind shear and maximum temperature anomaly layers. The meridional convergence and divergence zones coincide with the maximum zonal flow areas only at the pressure levels between 10 and 30 hPa where the high intensity of the zonal wind maxima produces a sharp vertical decrease (or increase) of the zonal flow. This spatial distribution determines the downward propagation of the QBO signal in the meridional wind. Thus areas of divergence and convergence descend linked to the maximum zonal wind shear center. On the other hand, although the area of influence of the meridional wind QBO signal is mainly centered between ±20° latitude, it can reach ±60° latitude for the most intense convergence and divergence centers.

[26] The QBO signal obtained for the stratospheric temperature is characterized by warm (cold) anomalies over the equator associated with westerly (easterly) shear zones. These anomalies change their sign at about ±15° latitude. Adiabatic descent (ascent) of air mass produces these warm (cold) anomalies required by the thermal wind balance. Variations in the temperature field also affect the layer thickness, causing anomalies in the geopotential height field of the same sign.

[27] Meridional flows can not be understood without the vertical motions related to temperature anomalies. Together, they form circulation cells that descend from the middle to the lower stratosphere. The intensity and location of these circulation cells are determined by the zonal wind shear layers produced by the succession of westerly and easterly wind zones for consecutive vertical levels. Summing up, this paper describes a coherent and mutually consistent signal of the QBO cycle in the stratospheric zonal and meridional wind, temperature, and geopotential height, associated with the secondary meridional circulation.

References

Baldwin, M. P., and T. J. Dunkerton (1998), Quasi-biennial modulation of the Southern Hemisphere stratospheric polar vortex, *Geophys. Res. Lett.*, *25*, 3343–3346.

Baldwin, M. P., and T. J. Dunkerton (1999), Downward propagation of the Arctic Oscillation from the stratosphere to the troposphere, *J. Geophys. Res.*, *104*, 30,937–30,946.

Baldwin, M. P., and T. J. Dunkerton (2001), Stratospheric harbingers of anomalous weather regimes, *Science*, *244*, 581–584.

Baldwin, M. P., et al. (2001), The Quasi-Biennial Oscillation, *Rev. Geophys.*, *39*, 179–229.

Choi, W., H. Lee, W. B. Grant, J. H. Park, J. R. Holton, K. M. Lee, and B. Naujokat (2002), On the secondary meridional circulation associated with the quasi-biennial oscillation, *Tellus*, *Ser. B*, *54*(4), 395–406.

Cordero, E. C., and T. R. Nathan (2000), The influence of wave- and zonal mean-ozone feedbacks on the quasi-biennial oscillation, *J. Atmos. Sci.*, *57*(20), 3426–3442.

Gray, L. J., S. J. Phipps, T. J. Dunkerton, M. P. Baldwin, E. F. Drysdale, and M. R. Allen (2001), A data study of the influence of the equatorial upper stratosphere on Northern-Hemisphere stratospheric sudden warmings, *Q. J. R. Meteorol. Soc.*, *127*, 1985–2003.

Hamilton, K. (1998), Dynamics of the tropical middle atmosphere: A tutorial review, *Atmos. Ocean*, *36*, 319–354.

Hamilton, K., and W. W. Hsieh (2002), Representation of the quasi-biennial oscillation in the tropical stratospheric wind by nonlinear principal component analysis, *J. Geophys. Res.*, *107*(D15), 4232, doi:10.1029/2001JD001250.

Holton, J. R. (1972), *An Introduction to Dynamic Meteorology*, 319 pp., Academic, San Diego, Calif.

Holton, J. R., and H. C. Tan (1980), Influence of the equatorial quasi-biennial oscillation on the global circulation at 50 Mb, *J. Atmos. Sci.*, *37*(10), 2200–2208.

Huesmann, A. S., and M. H. Hitchman (2001), Stratospheric quasi-biennial oscillation in the NCEP reanalyses: Climatological structures, *J. Geophys. Res.*, *106*, 11,859–11,874.

Huesmann, A. S., and M. H. Hitchman (2003), The 1978 shift in the NCEP reanalysis stratospheric quasi-biennial oscillation, *Geophys. Res. Lett.*, *30*(2), 1048, doi:10.1029/2002GL016323.

James, I. N. (1994), *Introduction to Circulating Atmosphere*, 422 p., Cambridge Univ. Press, New York.

Kalnay, E., et al. (1996), The NCEP/NCAR 40-year reanalysis project, *Bull. Am. Meteorol. Soc.*, *77*, 437–471.

Kinnersley, J. S., and K. K. Tung (1998), Modeling the global interannual variability of ozone due to the equatorial QBO and to extratropical planetary wave variability, *J. Atmos. Sci.*, *55*(8), 1417–1428.

Kinnersley, J. S., and K. K. Tung (1999), Mechanisms for the extratropical QBO in circulation and ozone, *J. Atmos. Sci.*, *56*(12), 1942–1962.

Kistler, R., et al. (2001), The NCEP-NCAR 50-year reanalysis: Monthly means CD-rom and documentation, *Bull. Am. Meteorol. Soc.*, *82*, 247–267.

Mann, M. E., and J. Park (1999), Oscillatory spatiotemporal signal detection in climate studies: A multiple-taper spectral domain approach, *Adv. Geophys.*, *41*, 1–131.

Maruyama, T. (1997), The quasi-biennial oscillation (QBO) and equatorial waves—A historical review, *Pap. Meteorol. Geophys.*, *48*, 1–17.

Naito, Y. (2002), Planetary wave diagnostics on the QBO effects on the deceleration of the polar-night jet in the Southern Hemisphere, *J. Meteorol. Soc. Jpn.*, *80*, 985–995.

Naujokat, B. (1986), An update of the observed quasi-biennial oscillation of the stratospheric winds over the tropics, *J. Atmos. Sci.*, *43*(17), 1873–1877.

Percival, D. B., and A. T. Walden (1993), *Spectral Analysis for Physical Applications: Multitaper and Conventional Univariate Techniques*, Cambridge Univ. Press., New York.

Plumb, R. A., and R. C. Bell (1982), A model of the quasi-biennial oscillation on an equatorial beta-plane, *Q. J. R. Meteorol. Soc.*, *108*, 335–352.

Reed, R. J. (1964), A tentative model of the 26-month oscillation in tropical latitudes, *Q. J. R. Meteorol. Soc.*, *90*, 441–446.

Ribera, P., and M. E. Mann (2002), Interannual variability in the NCEP reanalysis 1948–1999, *Geophys. Res. Lett.*, *29*(10), 1494, doi:10.1029/2001GL013905.

Ribera, P., and M. E. Mann (2003), ENSO related variability in the Southern Hemisphere, 1948–2000, *Geophys. Res. Lett.*, *30*(1), 1006, doi:10.1029/2002GL015818.

Ribera, P., D. Gallego, C. Peña-Ortiz, L. Gimeno, R. Garcia-Herrera, E. Hernandez, and N. Calvo (2003), The stratospheric QBO signal in the NCEP reanalysis, 1958–2001, *Geophys. Res. Lett.*, *30*(13), 1691, doi:10.1029/2003GL017131.

Salby, M., and P. Callaghan (2000), Connection between the solar cycle and the QBO: The missing link, *J. Clim.*, *13*, 2652–2662.

Thompson, D. W. J., M. P. Baldwin, and J. M. Wallace (2002), Stratospheric connection to Northern Hemisphere wintertime weather: Implications for prediction, *J. Clim.*, *15*, 1421–1428.

Venegas, S. A. (2001), *Statistical Methods for Signal Detection in Climate, DCESS Rep. 2*, Dan. Cent. for Earth Syst. Sci., Copenhagen.

D. Gallego, C. Peña-Ortiz, and P. Ribera, Departamento de Ciencias Ambientales, Universidad Pablo de Olavide, Carretera de Utrera, km 1, Sevilla, E-41013 Spain. (dgalpuy@dex.upo.es; cpenort@dex.upo.es; pribrod@dex.upo.es)

R. Garcia-Herrera and E. Hernández, Departamento Fisica de la Tierra II, Universidad Complutense de Madrid, Madrid, E-28040 Spain. (rgarcia@6000aire.fis.ucm.es; emiliano@6000aire.fis.ucm.es)

L. Gimeno, Departamento Fisica Aplicada, Universidad de Vigo, Facultad de Ciencias de Ourense, Ourense, E-32004 Spain. (l.gimeno@uvigo.es)